The Astrophysical Journal, 727:33 (13pp), 2011 January 20 doi:10.1088/0004-637X/727/1/33

STUDIES OF DIFFUSE INTERSTELLAR BANDS V. PAIRWISE CORRELATIONS OF EIGHT STRONG DIBs AND NEUTRAL HYDROGEN, MOLECULAR HYDROGEN, AND COLOR EXCESS

Scott D. Friedman[1], Donald G. York[2], Benjamin J. McCall[3], Julie Dahlstrom[4], Paule Sonnentrucker[1,5], Daniel E. Welty[6], Meredith M. Drosback[7], L. M. Hobbs[2,8], Brian L. Rachford[9], and Theodore P. Snow[10]
[1] Space Telescope Science Institute, Baltimore, MD 21218, USA; friedman@stsci.edu
[2] Department of Astronomy and Astrophysics and the Enrico Fermi Institute, University of Chicago, Chicago, IL, USA
[3] Departments of Chemistry, Astronomy, and Physics, University of Illinois at Urbana-Champaign, IL, USA
[4] Department of Physics and Astronomy, Carthage College, Kenosha, WI, USA
[5] Department of Physics and Astronomy, Johns Hopkins University, Baltimore, MD, USA
[6] Department of Astronomy, University of Illinois at Urbana-Champaign, IL, USA
[7] Department of Astronomy, University of Virginia, Charlottesville, VA, USA
[8] Yerkes Observatory, University of Chicago, Williams Bay, WI, USA
[9] Department of Physics, Embry-Riddle Aeronautical University, Prescott, AZ, USA
[10] Center for Astrophysics and Space Astronomy, University of Colorado, Boulder, CO, USA
Received 2010 June 16; accepted 2010 November 11; published 2010 December 29

ABSTRACT

We establish correlations between equivalent widths of eight diffuse interstellar bands (DIBs), and examine their correlations with atomic hydrogen, molecular hydrogen, and E_{B-V}. The DIBs are centered at λλ 5780.5, 6204.5, 6283.8, 6196.0, 6613.6, 5705.1, 5797.1, and 5487.7, in decreasing order of Pearson's correlation coefficient with N(H) (here defined as the column density of neutral hydrogen), ranging from 0.96 to 0.82. We find the equivalent width (EW) of λ5780.5 is better correlated with column densities of H than with E_{B-V} or H_2, confirming earlier results based on smaller data sets. We show that the same is true for six of the seven other DIBs presented here. Despite this similarity, the eight strong DIBs chosen are not correlated well enough with each other to suggest they come from the same carrier. We further conclude that these eight DIBs are more likely to be associated with H than with H_2, and hence are not preferentially located in the densest, most UV shielded parts of interstellar clouds. We suggest that they arise from different molecules found in diffuse H regions with very little H_2 (molecular fraction $f < 0.01$). Of the 133 stars with available data in our study, there are three with significantly weaker λ5780.5 than our mean H–λ5780.5 relationship, all of which are in regions of high radiation fields, as previously noted by Herbig. The correlations will be useful in deriving interstellar parameters when direct methods are not available. For instance, with care, the value of N(H) can be derived from W_λ(5780.5).

Key words: ISM: lines and bands – ISM: molecules

1. INTRODUCTION

The diffuse interstellar bands (DIBs) represent a long standing, spectroscopic mystery: hundreds of weak absorption features detected in the optical wavelength range remain unidentified (see Herbig 1995; Snow 1995, 2001 for summaries). While they were noted in stellar spectra as early as 1919 (Heger 1922), the DIBs had their suspected interstellar nature demonstrated more than a decade later (Merrill 1936).

Most of the early hypotheses regarding the progenitors (carriers) of DIBs centered on molecules, but by the early 1970s solid-state (i.e., grain) carriers were thought to be more likely (Herbig 1975). Molecules were re-introduced in the mid-1970s (Danks & Lambert 1976; Douglas 1977; Smith et al. 1977), and now most researchers have adopted large molecules or their ions as the most likely candidates (see Herbig 1995 for a review). Efforts to match laboratory spectra with observed DIB profiles have not been successful. Tulej et al. (1998) reported a match between the laboratory spectrum of C_7^- and five narrow DIBs, but with improved laboratory and astronomical data this was subsequently shown to be incorrect (McCall et al. 2001). Motylewski et al. (2000) found a weak astronomical feature at approximately the same laboratory wavelength and profile as HC_5N^+. More recently, Krelowski et al. (2010) have suggested that the laboratory spectrum of HC_4H^+ closely matches a newly identified, weak DIB at 5068.8 Å. However, confirmation of these claims by a match with a second line in laboratory and astrophysical spectra has not yet been made. Thus, the carriers still remain unidentified.

The DIBs have, thus, become recognized as a new window into the chemistry of the interstellar medium—if we could only identify their carriers. Attempts to identify the DIBs have included (1) searches for molecules in the laboratory with the same spectroscopic signatures as the DIBs (Leach 1995; Herbig 1995; Allain et al. 1996; Salama et al. 1996, 1999; McCall et al. 2000), (2) modeling of the structures detected in some DIB profiles in terms of rotational excitation of gas-phase molecules (Cossart-Magos & Leach 1990; Sarre et al. 1995; Galazutdinov et al. 2002b, 2008), and (3) searches for correlations of DIBs with other interstellar parameters (Wampler 1963, 1966; Snow et al. 1977; Sneden et al. 1978; Wu et al. 1981; Herbig 1993; Jenniskens & Désert 1994; Sonnentrucker et al. 1997, 1999; Thorburn et al. 2003; Weselak et al. 2004, 2008).

Finally, searches for correlations between individual pairs of DIBs were also carried out for the purpose of finding whether some of the DIBs were better correlated with each other than other pairs of DIBs. The reasoning was that these studies could reveal sets of DIBs that came from the same or similar carriers. The works of Krelowski & Walker (1987), Josafatsson & Snow (1987), Westerlund & Krelowski (1989), Cami et al. (1997), and Weselak et al. (2001) led to the identification of "families" of DIBs. The DIB pair thought to show the best correlation

is comprised of the λ6196.0 and λ6613.6[11] DIBs (Cami et al. 1997; Moutou et al. 1999; Galazutdinov et al. 2002b). Since no observed correlation was perfect, agreement on which DIB belonged to which family, or whether pairs of DIBs arise from the same carrier, was not always reached when comparing these studies.

To address these issues we compiled a large spectral database toward approximately 200 stars, which has generated a series of papers on diverse properties of DIBs. Thorburn et al. (2003, Paper I) describe the relationship between C_2 and certain DIBs. Hobbs et al. (2008, 2009, Papers II and III) present spectral atlases of DIBs toward the spectroscopic binary star HD 204827 and toward HD 183143. McCall et al. (2010, Paper IV) revisited the λλ6196.0, 6613.6 correlation. The unprecedented data quality and statistics of our survey (see Section 2) show that this pair has the highest correlation of any known pair and the data would be consistent with a perfect correlation if the errors were underestimated by only a modest amount. In the present paper, we extend our investigation to more fully study the eight strong DIBs λλ 5780.5, 6204.5, 6283.8, 6196.0, 6613.6, 5705.1, 5797.1, and 5487.7, in order of decreasing Pearson's correlation coefficient with N(H).[12] We also examine the DIB–DIB correlations as well as the correlation of the DIBs with the column density of molecular hydrogen and with color excess.

This paper is organized as follows. In Section 2, we briefly describe how the survey data were obtained and reduced, and we present an extensive list of the line-of-sight parameters and DIB EWs toward the 133 stars reported here. In Section 3, we present a large variety of correlation coefficients and plots, and the slopes and intercepts of correlation plots between λ5780.5 with the other DIBs and with N(H), $N(H_2)$, and E_{B-V}. In Section 4, we discuss these results, including the importance of systematic errors which arise among measurements of DIB EWs. In Section 5, we summarize the results of this study.

2. OBSERVATIONS AND DATA ANALYSIS

From 1999 to 2002 we obtained a high signal-to-noise data set on DIBs in the spectra of about 200 stars spanning a large range of reddening, $E_{B-V} \sim 0.01$–3.31 mag (Papers I, II, and III), and their associated diatomic or triatomic molecules (Oka et al. 2003). The reader is referred to those papers for details, and we give only a brief description of the data analysis here. The echelle spectrograph (Wang et al. 2003) was used on the Apache Point Observatory 3.5 m telescope to obtain spectra at a resolving power $\lambda/\Delta\lambda = 38{,}000$ from 3600 Å to 9000 Å at a nominal signal-to-noise ratio of roughly 1000 at 5780 Å for each sight line (see Paper I). Stellar lines are distinguished from DIBs in reddened stars by comparison with stars of the same spectral type but with low reddening. Telluric lines are removed by use of a complex scheme that measures patterns of behavior in key telluric absorption lines and makes a blanket correction for each observation, depending on air mass and humidity. DIBs that were generally uncontaminated by stellar and telluric blends were measured as described extensively in Papers I and II.

DIB absorption features pose special challenges for any study, such as this one, seeking to quantify EWs. Ultimately, the goal of DIB EW measurements must be to include all blended absorption from the same chemical species without including blended absorption from other chemical species. However, correctly distinguishing contaminating features from those belonging to the same compound itself presupposes knowledge of those chemical species and their spectra. As long as the DIBs carriers remain unidentified, the shape and width of the spectral profiles will remain uncertain. The band structure could be due either to blending with features from other carriers or to blending with features from higher rotational levels of the same species, or could be due to both types of blends.

For this study, and for the previous papers in this series, continuum normalization was accomplished by use of eighth-order Legendre polynomials. For the broadest DIBs, absorption spanned multiple spectral orders. In these cases, continuum profiles were estimated by interpolation across multiple orders. EWs were hand-measured by one of us (J.D.), along with inspection of each DIB in comparison with nearly unreddened standard stars in order to identify stellar lines. Limits of integration were set by where the DIB absorption recovered to the continuum. Where the profile did not fully recover to the continuum, we set the limits at inflection points in the profile, which often indicate an appropriate endpoint (Krelowski & Sneden 1993). We made no assumption that the line shapes have Gaussian profiles. EWs were computed with direct integration.

We do not presume that the present choices of integration endpoints are in any way definitive, nor do we suppose that any prior work has made similar choices with any more assurance of correctness or fewer reasonable arguments in favor of their choices. Integration endpoints chosen in the present study reflect a primary interest in *repeatable* measurements and minimal sensitivity to continuum location error, both of which are essential to reducing the scatter in correlations from measurement error but do not prevent scatter from other, less easily avoided causes. We do not recommend that the present EWs be combined from those reported in studies by other investigators without carefully considering the specific definitions of what constitutes the measurement criteria for each diffuse band.

The quantity used to investigate correlations differs from study to study, even among the same investigators. For example, Moutou et al. (1999) used central depths, stating that they are less sensitive to contamination than are EWs, although they point out that depths reflect well the correlation in EW. Weselak et al. (2001) find in their study that central depths correlate better than EWs. On the other hand, in a study at very high spectral resolution (220,000) of the profiles of λλ6196, 6614, Galazutdinov et al. (2002a) found a correlation in the EWs of the DIBs but not in the FWHMs. The FWHM of λ6196 varies by 50% over the seven sight lines sampled, whereas for λ6614 it is nearly constant within observational errors. The substructure of both profiles varies among the sight lines but in an unrelated way for the two DIBs. Interstellar atomic lines do not reveal Doppler broadening, so the authors believe the absorption arises in a single cloud.

Until the identification of DIBs is secure, by definitive matches with laboratory spectra, no single method can be

[11] Due to uncertainty in the rest wavelength of DIBs, and differing practices by various authors for truncating or rounding wavelengths, the nomenclature of DIBs in the literature is confusing. Indeed, with the increasing number of known DIBs (Hobbs et al. 2008, 2009) quoting wavelengths to only integer values can be ambiguous. Therefore, we use the wavelengths that are tabulated in Table 2 of the Hobbs et al. (2008) study of HD 204827, and round to five significant figures. For the three narrow DIBs, λλ5780.5, 6613.6, and 5797.1, the central wavelength found by Hobbs et al. (2009) for HD 183143 are 0.1 Å longward of the wavelengths given here. This may be the result of component structure differences in the velocity profiles for these sight lines.

[12] We represent the column density of neutral atomic hydrogen by N(H). This is often mistakenly denoted N(H I). However, H I actually denotes the spectral line of atomic hydrogen.

deemed superior. We have elected to base our correlation studies on measurements of EWs rather than FWHM or the central depths of profiles. While the latter two measures are less likely to suffer from contamination by nearby, unrelated species, they will fail to account for broad absorption due to *R*- or *P*-branch transitions, for example. The strength of these branches depends on the unknown rotation temperature of the molecules along the line of sight, which can vary from cloud to cloud, and even within a cloud. As shown in Figure 1 of Oka et al. (2003), the absorption can occur over a rather large wavelength interval. Another reason to use EWs rather than central depth is that most of these sight lines intersect multiple clouds, so our results represent averages over the intervening clouds. Doppler splitting could affect measures of central depth, especially for narrow DIBs. As long as there is not saturated component structure, EWs will not suffer from this error. Finally, measures of EWs are independent of the resolution of the instrument used, which is not true of FWHM or central depth.

Standard techniques were used for cosmic ray removal, flat fielding, background and bias subtraction, and extraction to one dimensional spectra. The spectra from adjacent orders were co-added to give a blazeless spectrum. A set of 35 lines that were most free of stellar blending or telluric line contamination were initially measured. The estimates of correlations among DIBs and between DIBs and other interstellar quantities are based on DIB measurements presented by Paper I for an expanded set of stars, on the H and H_2 column densities of Rachford et al. (2002, 2009), and on color excess values collected from the literature by one of us (LMH) based on the color scale of Johnson (1963). Errors on each data point were estimated by measurements in adjacent parts of the continuum, free of other DIBs and of stellar or telluric lines, and then were propagated through the analysis. One sigma errors are used throughout. McCall et al. (Paper IV) give an extensive discussion of additional errors that may affect the data. They suggest that our errors may be underestimated by about a factor of two due to systematic effects, the three most likely of which are continuum placement errors, the possible presence of unidentified weak DIBs close to the DIBs being measured, and the residual errors arising from imperfect removal of telluric water vapor lines. In the present study, however, we use the formally propagated errors described in Paper I.

Table 1 includes a list of all 133 stars in this study, their spectral types and luminosity class, N(H), $N(H_2)$, E_{B-V}, and the EWs of the eight DIBs we focus on here. This analysis excludes the 17 lines noted as being correlated with C_2 (Paper I) and C_3 (Oka et al. 2003), whose relationships with K I, CO, CH, and other molecular species will be the subject of a future study by our group. Rachford et al. (2009) did a reanalysis of N(H) and $N(H_2)$ along some of the sight lines included in the current study. The values that they found of these quantities differ from those derived in the original analysis by less than 1σ in all cases, much less than the cosmic dispersion of these quantities. We therefore use the results of our original, homogeneous data analysis, as presented by Rachford et al. (2002).

3. DIB PROFILES AND CORRELATION PROPERTIES

The DIBs chosen for this study were meant to avoid the broadest DIBs, for which our echelle measurements can underestimate the line strengths (Hobbs et al. 2009) due to continuum placement difficulties. They were also meant to focus on the classic strong DIBs, which do not include the C_2 DIBs found by Thorburn et al. in Paper I. The strongest DIBs with FWHM less than that of λ5780.5 are included (λλ5797.1, 6613.6). The DIB at λ6283.8 is the second strongest DIB after λ4428.1, so it was included to test for any evidence of saturation in the range of E_{B-V} for our stars, even though it has FWHM = 4.77 Å (Table 2). Another much weaker DIB, λ5487.7, was included as a comparison. Two lines were included because of their previously known correlations with other DIBs: λ5705.1 (used in Paper I to test for saturation in λ5780.5) and λ6196.0, previously noted for its close correlation with λ6613.6. An eighth line (λ6204.5) was included since it has two narrow components that are blended and it is not clear if they should be measured together or separately. This characteristic is shared by other DIBs, such as λ5849.8 and λ6660.7, but we selected λ6204.5 because it is among the strongest DIBs. The DIBs in Paper I were analyzed with respect to their correlation with each other. The DIBs chosen for this paper are at the high end of correlation coefficients and include all the moderately well correlated DIBs. All other DIBs from Paper I are less well correlated with each other than those in this paper.

Spectral profiles of these eight DIBs toward HD 183143 and HD 204827 are shown in Figure 1. HD 183143 has been observed by many DIB investigators (e.g., Herbig 1975; Jenniskens & Désert 1994; Tuairisg et al. 2000) and is the basis for the atlas discussed in Paper III. HD 204827, discussed in Paper II, reveals several narrow, weak DIBs which are not evident in HD 183143, and vice versa. Some broad DIBs are not seen in common in the two stars, as well. We note that the central wavelength for each band in Figure 1 is slightly longer for HD 183143 than for HD 204827, a systematic difference anticipated and discussed in some detail in Papers II and III. The unavoidable uncertainty in the precise zero point for DIB wavelengths arises primarily from the combination of the multiple interstellar clouds present along both stellar lines of sight and the unknown identities and laboratory spectra of the molecules presumed to cause the DIBs. The median offset for the eight bands in Figure 1 corresponds to about 7 km s^{-1}. Had we arbitrarily chosen to assign the laboratory K I wavelength to the mid-point between the two main components of the interstellar K I line toward HD 183143 (Paper III, Figure 2), for example, this systematic median offset would effectively be removed. This result implies that the DIBs show component structure. Indeed, Doppler splitting in the narrow DIB λ6196.0, matching the splitting of interstellar K I, about 15 km s^{-1}, was observed in high-resolution spectra of HD 183143 by Herbig & Soderblom (1982). However, in our observations the scatter in the mean is such that some DIBs may be dominant in one component and some in others. The offsets for the narrowest DIBs are clear. We will address this issue in a future paper (D. G. York et al. 2011, in preparation).

Figure 1 also illustrates our choice of integration limits for the DIBs along these two sight lines, and the ambiguities this involves. For example, λ5780.5 is either at the bottom of a broad feature or else is flanked by a series of narrow, possibly related, features. Not knowing the origin of each feature, we assumed the former interpretation as did, for example, Galazutdinov et al. (2004). For λ6204.5 we include the extended red wing. Porceddu et al. (1991) conclude that λ6205 is a separate DIB on the basis of a varying central depth ratio of the two features. They further conclude that these differences are due to differences in the physical parameters within a single interstellar cloud, based on the lack of observed Doppler splitting in the narrow λ6196.0 DIB, at their moderate resolving power (30,000) and SNR (200–300). For λ5797.1 we include the blue wing, in contrast to Galazutdinov et al. (2004), who believe it is blended

Table 1
Stellar Properties, Interstellar Line Data, and DIB Equivalent Widths (mÅ)

HD	Sp Type	E_{B-V}[a]	log(N(H))	log(N(H_2))	References[b]	5487.7	5705.1	5780.5	5797.1	6196.0	6204.5	6283.8	6613.6
2905	B1Iae	0.33	21.26 ± 0.09	20.27 ± 0.09	3,6	69 ± 3	66 ± 7	314 ± 5	110 ± 5	35 ± 2	116 ± 8	665 ± 65	130 ± 4
10516	B2Vep	0.20		19.08 ± 0.09	–,6	<10	<15	67 ± 4	23 ± 4	5.4 ± 1	23 ± 5	<200	11 ± 1
11415 (ϵ Cas)	B3III	0.05				<20	<6	71 ± 2	<8	<2	<12	55 ± 15	1.8 ± 0.6
16219	B5V	0.04				<15	<12	36 ± 6	12 ± 4	3 ± 0.8	13 ± 4.5	146 ± 40	<6
19374	B1.5V	0.13	21.06 ± 0.11		1,–	17 ± 3	36 ± 5	138 ± 6	41 ± 5	12 ± 1	51.5 ± 5	428 ± 45	42 ± 3
20041	A0Ia	0.72				109 ± 5	101 ± 7	429 ± 6	161 ± 6	54 ± 2	179 ± 9	1030 ± 60	245 ± 5
21071	B7V	0.05				14 ± 3	24 ± 4	91 ± 5	38 ± 5	7.6 ± 0.8	30.5 ± 4.5	202 ± 45	23.5 ± 2
21483	B3III	0.56				56 ± 10	35 ± 10	181 ± 7	96 ± 6	22.5 ± 1.5	71 ± 5	397 ± 45	89 ± 4
21389	A0Iae	0.57				79 ± 5	104 ± 7	411 ± 8	160 ± 7	41.7 ± 2	184 ± 9	1211 ± 80	161 ± 4
22951 (40 Per)	B0.5V	0.27	21.04 ± 0.11	20.46 ± 0.09	5,6	33 ± 4	41 ± 4	115 ± 5	52 ± 6	16.7 ± 1.5	58 ± 6	337 ± 40	49 ± 2
23180 (o Per)	B1III	0.31	20.82 ± 0.09	20.61 ± 0.09	1,6	31 ± 7	45 ± 6	101 ± 7	81.6 ± 6	12.7 ± 1	36 ± 7	200 ± 60	51 ± 3
281159	B5V	0.85	21.38 ± 0.3	21.09 ± 0.19	8,8	57 ± 7	68 ± 10	310 ± 5	120 ± 6	32 ± 1	107 ± 6	737 ± 80	151 ± 5
23408	B8III	0.02		19.75 ± 0.13	–,6	<10	<15	<25	<5	2.7 ± 0.8	<9	<120	7 ± 1.5
23480	B6IVe	0.08		20.11 ± 0.09	–,6	<10	<15	31 ± 5	<5	<2.5	<10	116 ± 30	<4
24398 (ζ Per)	B1Ib	0.31	20.8 ± 0.08	20.68 ± 0.09	1,6	43 ± 7	36 ± 10	114 ± 7	77 ± 5	16.2 ± 1	38 ± 7	185 ± 50	66 ± 5
24534(X Per)	O9.5pe	0.59	20.73 ± 0.06	20.92 ± 0.04	1,8	22 ± 5	<30	98 ± 8	68 ± 4	14.7 ± 1	38 ± 4	270 ± 60	72 ± 5
24760	B0.5V+A2	0.10	20.45 ± 0.11	19.52 ± 0.13	1,6	<12	<20	81 ± 5	22 ± 4	7.3 ± 1	34 ± 5	283 ± 40	19.5 ± 2
24912	O7e	0.33	21.05 ± 0.08	20.54 ± 0.08	1,6	41 ± 5	24 ± 7	209 ± 7	46 ± 7	21 ± 1	95 ± 6	507 ± 60	79 ± 3
26571	B9IIIp	0.25				<15	48 ± 7	151 ± 7	82.6 ± 10	20 ± 2.5	53 ± 10	273 ± 40	83 ± 3
27778	B3V	0.37		20.79 ± 0.06	8,8	<20	17 ± 3	86 ± 4	39 ± 2	11.5 ± 0.5	34 ± 3	170 ± 50	44 ± 2
28375	B3V	0.10				<12	18 ± 5	66 ± 5	23 ± 5	5.5 ± 0.8	20 ± 5	202 ± 45	19.5 ± 2
28497	B1Ve	0.03	20.23 ± 0.1	15.09 ± 0.1	3,11			13 ± 4	<9	<3	<15	<120	<5
29647	B8IIIp	1.00				<12	<24	70 ± 7	39 ± 5	9.7 ± 1.4	20 ± 5	95 ± 25	57 ± 2
30614	O9.5Iae	0.30	20.97 ± 0.09	20.34 ± 0.08	1,6	35 ± 5	54 ± 10	133 ± 5	56 ± 3	17.2 ± 1.5	63.7 ± 6	360 ± 60	71.5 ± 5
34078 (AE Aur)	O9.5Ve	0.52	21.2 ± 0.11		1,–	48 ± 5	48 ± 3	181 ± 5	56 ± 3	23 ± 1	111 ± 4	510 ± 80	61 ± 2
34503	B5III	0.05						25 ± 5	<12	<3	<15	145 ± 45	<6
34798	B3V	0.04						12 ± 4	9 ± 3	<5	<25	160 ± 40	<7
35149	B1V	0.11	20.56 ± 0.07	18.3 ± 0.11	1,9	12.7 ± 3.5	<12	57 ± 3	15.7 ± 3	5.5 ± 0.7	22.6 ± 4	286 ± 45	21.7 ± 2
36512	B0V	0.04	20.27 ± 0.11		1,–			25 ± 5	<9	<12	<25	155 ± 40	10 ± 2
36486	B0III+O9V	0.08	20.19 ± 0.05	14.74 ± 0.05	12,13			23 ± 5	<15	3.1 ± 0.8	<20	150 ± 45	<5
36591	B1IV	0.07				13 ± 4	<15	28 ± 6	<10	3.5 ± 1	26 ± 8	173 ± 45	10 ± 2
36371	B5Iab	0.43				88 ± 7	72 ± 5	313 ± 7	127 ± 7	37.5 ± 2	137 ± 10	743 ± 60	145 ± 4
36822 (ϕ^1 Ori)	B0III	0.14	20.84 ± 0.07	19.32 ± 0.07	1,6	29 ± 6	25 ± 6	68 ± 6	31 ± 5	7.2 ± 0.8	36 ± 8	271 ± 45	24 ± 3
36861	O8e	0.15	20.81 ± 0.12	19.12 ± 0.1	1,6			50 ± 5	26 ± 4	5.6 ± 0.8	41 ± 5	228 ± 40	19 ± 2
37021 (θ^1 Ori B)	B0V	0.54				20 ± 5	<18	61 ± 6	<15	<4	49 ± 9	432 ± 70	6.2 ± 1.5
37022 (θ^1 Ori C)	O6	0.34	21.54 ± 0.11	15.65 ± 0.13	1,7	8 ± 2.5	23 ± 6	76 ± 6	19 ± 6	4.5 ± 0.7	55 ± 7	468 ± 70	9 ± 2.5
37043	O9III	0.07	20.2 ± 0.1	14.69 ± 0.11	1,7	<15	<30	34 ± 6	<12	3.5 ± 1	21 ± 5	<120	5 ± 1.5
37061	B1V	0.52	21.81 ± 0.07		3,–	33 ± 4	46 ± 5	169 ± 7	35 ± 5	12.6 ± 1.5	103 ± 6	675 ± 55	34.4 ± 3
37128	B0Iae	0.05	20.48 ± 0.11	16.28 ± 0.2	1,9			18 ± 3	<5	4 ± 1	21 ± 5	128 ± 40	6.8 ± 1.4
37367	B2IV-V	0.40				95 ± 9	94 ± 8	454 ± 5	133 ± 6	40 ± 1	154 ± 9	1117 ± 60	144 ± 4
37742	O9.5Ibe	0.06	20.39 ± 0.09	15.88 ± 0.11	1,9			31 ± 4	<6	2.8 ± 0.8	38 ± 5	<90	6.2 ± 1.5
37903	B1.5V	0.35	21.17 ± 0.1	20.92 ± 0.06	1,10	46 ± 8	36 ± 5	183 ± 10	33 ± 5	11.5 ± 1.5	56.6 ± 6	503 ± 70	36 ± 4
38087	B5V	0.29		20.64 ± 0.07	–,10	<25	<30	162 ± 6	44 ± 6	12.6 ± 1	35 ± 6	325 ± 45	54 ± 3
38771	B0.5Ia	0.05	20.6 ± 0.08	15.68 ± 0.14	1,7			33 ± 5	15 ± 4	5 ± 0.8	25 ± 5	126 ± 35	7.7 ± 1.5
39777	B1.5V	0.07						25 ± 6	<10	<6	<25	156 ± 45	<10
40111	B0.5II	0.20	21.03 ± 0.09	19.73 ± 0.1	1,6	47 ± 10	44 ± 8	169 ± 6	44 ± 5	16.3 ± 1	74 ± 7	428 ± 50	37 ± 2
40893	B0IV	0.46	21.50 ± 0.10	20.58 ± 0.06		78 ± 6	80 ± 7	391 ± 5	109 ± 6	39 ± 1.5	203 ± 9	1030 ± 75	151 ± 4
41117	B2Iae	0.45	21.4 ± 0.15	20.69 ± 0.1	1,10	89 ± 6	86 ± 5	356 ± 10	148 ± 8	42 ± 1	135 ± 5	760 ± 100	154 ± 3
42087	B2.5Ibe	0.36	21.4 ± 0.11	20.52 ± 0.12	1,10	72 ± 5	75 ± 6	275 ± 7	99 ± 2	30 ± 1	115 ± 4	675 ± 70	115 ± 3
43247	B9II-III	0.03				19 ± 4	19 ± 5	64 ± 6	25 ± 5	8 ± 1	34 ± 4	190 ± 40	23 ± 2.5
43384	B3Ib	0.58	21.27 ± 0.30	20.87 ± 0.14	–,10	109 ± 7	113 ± 4	455 ± 7	155 ± 5	48 ± 1	170 ± 6	950 ± 50	194 ± 3
46056	O8V	0.50	21.38 ± 0.14	20.68 ± 0.06	1,10	66 ± 7	90 ± 10	300 ± 7	135 ± 9	32 ± 1.5	151 ± 9	750 ± 60	137 ± 4
46202	O9V	0.49	21.58 ± 0.15	20.68 ± 0.07	1,10	55 ± 5	76 ± 10	332 ± 6	119 ± 8	35 ± 3	159 ± 10	935 ± 70	136 ± 3
46711	B3II	1.04				187 ± 15	173 ± 15	820 ± 10	269 ± 8	83 ± 4	287 ± 14	1500 ± 150	363 ± 5
47129	O8V+O8f	0.36	21.18 ± 0.11	20.55 ± 0.09	1,6	46 ± 7	30 ± 8	204 ± 5	89 ± 4	24 ± 1.5	93 ± 6	550 ± 50	89 ± 4
47839	O7Ve	0.07	20.31 ± 0.1	15.55 ± 0.09	1,7			30 ± 3	7 ± 2	<3	12 ± 5	45 ± 15	
48099	O6e	0.27	21.2 ± 0.12	20.29 ± 0.07	1,7	33 ± 4	43 ± 5	207 ± 7	52 ± 6	19.2 ± 0.8	87 ± 5	595 ± 50	78 ± 2
50064	B6Ia	0.85				190 ± 12	154 ± 12	693 ± 10	288 ± 15	72 ± 5	280 ± 12	1415 ± 150	275 ± 6
51309	B3II	0.11				19 ± 6	17 ± 5	56 ± 5	17 ± 5	6.3 ± 1	24 ± 5	319 ± 50	11 ± 2
53367	B0IVe	0.74	21.32 ± 0.30	21.04 ± 0.05	–,10	39 ± 7	40 ± 6	175 ± 5	86 ± 5	23 ± 1.5	102 ± 9	542 ± 60	81 ± 3
53975	O8V	0.21	21.1 ± 0.08	19.23 ± 0.09	1,6	41 ± 5	36 ± 5	177 ± 5	26 ± 6	16 ± 1	92 ± 7	607 ± 60	45 ± 4
54662	O7III	0.35	21.23 ± 0.1	20 ± 0.09	1,6	42 ± 5	42 ± 6	217 ± 7	52 ± 8	24.5 ± 1.5	100 ± 7	595 ± 60	93 ± 4
57060	O7e+O7	0.17	20.78 ± 0.1	15.78 ± 0.1	1,7	23 ± 7	<15	62 ± 4	<25	7.8 ± 1	44 ± 9	240 ± 50	14 ± 2
57061 (τ CMa)	O9III	0.16	20.8 ± 0.08	15.45 ± 0.13	1,7	<20	16 ± 5	63 ± 4	<20	6.6 ± 0.8	56 ± 5	272 ± 45	11 ± 2
90994	B6V	0.00						14 ± 3	<12	<2.5	<15	<150	<6
91316	B1Ib	0.05	20.44 ± 0.09	15.58 ± 0.08	1,6	<20	12 ± 3	38 ± 3	17 ± 3	3.6 ± 0.6	20 ± 5	75 ± 20	10 ± 3
97991	B1.5V	0.04	20.54 ± 0.08	15.99 ± 0.2	1,11			32 ± 6	16 ± 5	<4	<30	135 ± 45	9.5 ± 2.5
143018	B1V+B2V	0.05	20.66 ± 0.1	19.32 ± 0.1	1,6	<20	<18	39 ± 4	7 ± 2	2.5 ± 0.8	14 ± 5	145 ± 40	10 ± 2
143275	B0.3IV	0.17	21.01 ± 0.08	19.42 ± 0.1	1,6	27 ± 5	19 ± 6	82 ± 5	26 ± 4	7.8 ± 0.8	30 ± 4	250 ± 25	23 ± 3
144217 (β^1 Sco AB)	B1V	0.19	21.03 ± 0.08	19.83 ± 0.04	1,6	28 ± 9	39 ± 5	171 ± 5	34 ± 4	13.2 ± 0.8	57.6 ± 5	397 ± 45	42 ± 3
144218 (β^2 Sco)	B2V	0.22				41 ± 9	44 ± 6	191 ± 5	36 ± 5	13 ± 1	62 ± 7	404 ± 45	47 ± 4
144470 (ω^1 Sco)	B1V	0.22	21.18 ± 0.08	20.06 ± 0.06	5,6	37 ± 8	37 ± 6	192 ± 5	40 ± 4	17 ± 1	58 ± 6	403 ± 40	63 ± 3
145502 (ν Sco AB)	B3V	0.24	21.2 ± 0.12	19.89 ± 0.07	1,6	26 ± 8	37 ± 7	187 ± 5	49 ± 5	16 ± 1	55 ± 6	421 ± 40	63 ± 3
147165 (σ Sco)	B2III+O9V	0.41	21.38 ± 0.08	19.79 ± 0.07	1,6	51 ± 5	64 ± 5	254 ± 5	54 ± 3	15.2 ± 0.7	75 ± 7	498 ± 50	63 ± 3

Table 1
(Continued)

HD	Sp Type	E_{B-V}[a]	log(N(H))	log(N(H_2))	References[b]	5487.7	5705.1	5780.5	5797.1	6196.0	6204.5	6283.8	6613.6
147888	B5V	0.47	21.44 ± 0.30	20.47 ± 0.05	–,10	45 ± 5	54 ± 4	252 ± 12	60 ± 5	19 ± 1	56 ± 5	390 ± 60	82 ± 2
147889	B2V	1.07				75 ± 6	85 ± 6	377 ± 8	163 ± 5	46 ± 2	95 ± 7	530 ± 50	180 ± 5
147933 (ρ Oph A)	B2IV	0.48	21.63 ± 0.09	20.57 ± 0.07	1,6	55 ± 6	44 ± 8	222 ± 10	71 ± 6	17.1 ± 1	50 ± 7	426 ± 80	68 ± 5
148184	B2IVpe	0.52		20.63 ± 0.09	–,6			102 ± 5	64 ± 4	14 ± 1	55 ± 5	327 ± 45	40 ± 3
148605	B2V	0.13		18.74 ± 0.09	–,6	<15	<15	51 ± 4	12 ± 4	3.8 ± 1	15 ± 5	173 ± 45	9.4 ± 2
149404	O9Iae	0.68	21.4 ± 0.14		1,10	142 ± 10	94 ± 6	436 ± 8	112 ± 10	42 ± 1.5	158 ± 8	900 ± 60	170 ± 3
149881	B0.5III	0.10	20.57 ± 0.08	19.09 ± 0.1	1,6	<15	<18	44 ± 4	12 ± 3	4.8 ± 0.8	25 ± 5	147 ± 40	9 ± 1.5
149757	O9.5V	0.32	20.69 ± 0.1	20.66 ± 0.04	1,6	11 ± 3	<18	83 ± 7	38 ± 4	10 ± 1	36 ± 5	175 ± 35	41 ± 3
157857	O7e	0.51				40 ± 5	43 ± 5	265 ± 5	72 ± 5	28 ± 1	118 ± 8	905 ± 60	114 ± 5
159975	B8II-IIIp	0.19				32 ± 5	33 ± 4	189 ± 5	72 ± 4	17 ± 1	60 ± 5	500 ± 50	64 ± 3
162978	O8III	0.35	21.28 ± 0.08		1,–	42 ± 7	44 ± 8	211 ± 14	58 ± 9	21.5 ± 2	88 ± 11	558 ± 60	64 ± 5
164353	B5Ib	0.11	21	20.26 ± 0.14	5,6	24 ± 5	24 ± 4	124 ± 4	38 ± 4	12.9 ± 0.7	46 ± 5	378 ± 45	53 ± 3
164740 (Herschel 36)	O7.5V	0.87		20.19 ± 0.12	–,10	80 ± 9	119 ± 18	463 ± 8	102 ± 7	28 ± 2	142 ± 9	880 ± 75	132 ± 6
166734	O8e	1.39				216 ± 10	168 ± 9	727 ± 8	322 ± 15	93 ± 3	321 ± 12	1560 ± 200	401 ± 5
166937 (μ Sgr)	B8Iape	0.25				45.5 ± 3	63 ± 5	283 ± 4	100 ± 5	25.7 ± 1	90 ± 6	785 ± 70	90 ± 3
167971	O8e	1.08	21.6 ± 0.3	20.85 ± 0.12	8,8	116 ± 10	131 ± 5	512 ± 9	208 ± 6	58 ± 2	241 ± 10	1450 ± 200	219 ± 3
168076	O5f	0.78	21.65 ± 0.23	20.68 ± 0.08	1,8	110 ± 15	118 ± 12	541 ± 10	250 ± 8	59.5 ± 3	219 ± 15	1090 ± 150	221 ± 6
169454	B1.5Ia	1.12				128 ± 10	118 ± 5	510 ± 7	213 ± 5	57 ± 1	219 ± 10	1580 ± 170	205 ± 5
170740	B2V	0.48	21.04 ± 0.15	20.86 ± 0.08	1,8	66 ± 7	63 ± 5	255 ± 7	92 ± 5	26.6 ± 0.8	76 ± 4	595 ± 60	125 ± 4
172028	B2V	0.79				50 ± 10	53 ± 5	256 ± 8	217 ± 5	37 ± 1	94 ± 5	450 ± 60	137 ± 3
175156	B5II	0.31				24 ± 4	36 ± 4	151 ± 4	85 ± 5	18 ± 0.8	59 ± 6	418 ± 55	69 ± 4
179406	B3V	0.33	21.23 ± 0.15	20.73 ± 0.07	–,10	25 ± 5	29 ± 6	172 ± 5	76 ± 3	19.8 ± 0.7	44 ± 3	430 ± 60	98 ± 2
183143	B7Iae	1.27				225 ± 14	172 ± 7	761 ± 6	257 ± 8	89 ± 2	340 ± 11	1910 ± 30	332 ± 4
185418	B0.5V	0.50	21.11 ± 0.15	20.76 ± 0.05	8,8	57 ± 6	57 ± 3	273 ± 5	105 ± 5	35 ± 1	111 ± 6	640 ± 50	164 ± 4
186994	B0III	0.17	20.9 ± 0.15	19.59 ± 0.04	5,10	40 ± 6	<30	101 ± 5	23 ± 4	11 ± 1	60 ± 6	296 ± 40	17 ± 3
192639	O8e	0.66	21.32 ± 0.12	20.69 ± 0.05	1,8	75 ± 6	81 ± 5	324 ± 5	79 ± 7	39 ± 1	151 ± 5	817 ± 50	150 ± 3
194839	B0.5Ia	1.18				216 ± 16	153 ± 20	585 ± 6	186 ± 7	56 ± 2	289 ± 7	1690 ± 100	173 ± 4
Cyg OB2 5	O7f	1.99				251 ± 15	195 ± 20	774 ± 8	239 ± 12	83 ± 1	363 ± 10	1990 ± 200	312 ± 8
Cyg OB2 12	B5Ie	3.31				225 ± 30	214 ± 15	850 ± 20	381 ± 15	103 ± 3	395 ± 9	2215 ± 200	377 ± 6
198478	B3Iae	0.54				90 ± 6	72 ± 4	332 ± 5	112 ± 4	33.1 ± 1.5	130 ± 7	919 ± 60	139 ± 3
199579	O6Ve	0.37	21.04 ± 0.11	20.53 ± 0.04	1,8	32 ± 4	21 ± 3	128 ± 5	50 ± 4	15.5 ± 1	53 ± 2	315 ± 50	63 ± 2
199892	B7III	0.04						29 ± 9	<9	<3	16 ± 5	150 ± 45	<6
201345	O9.5V	0.18				46 ± 7	15 ± 5	100 ± 6	29 ± 5	8.9 ± 1	52 ± 6	385 ± 55	21 ± 3.5
202850	B9Iab	0.12				37 ± 7	47 ± 7	173 ± 6	55 ± 6	15 ± 1	82 ± 10	576 ± 50	42 ± 3
203938	B0.5IV	0.74	21.48 ± 0.15	21 ± 0.06	8,8	78 ± 6	68 ± 4	356 ± 5	152 ± 5	42 ± 1	151 ± 5	936 ± 60	146 ± 3
204172	B0Ib	0.16	21 ± 0.11	19.6 ± 0.09	5,6	43 ± 5	19 ± 5	120 ± 4	31.6 ± 3	12.1 ± 1	57.6 ± 4	322 ± 60	33 ± 2
204827	B0V	1.11				68 ± 4	58 ± 3	257 ± 4	199 ± 3	41.5 ± 1	116 ± 4	518 ± 60	171 ± 3
206165	B2Ib	0.47				60.5 ± 4	58 ± 5	231 ± 7	106 ± 5	26 ± 1	86 ± 6	486 ± 60	111 ± 3
206267	O6f	0.53	21.3 ± 0.15	20.86 ± 0.04	8,8	53 ± 7	59 ± 4	242 ± 7	102 ± 5	29 ± 1	103 ± 5	544 ± 45	126 ± 3
206773	B0Vpe	0.54				34 ± 7	20 ± 6	193 ± 6	71 ± 6	21.5 ± 1	67 ± 7	461 ± 60	90 ± 4
207198	O9IIe	0.62	21.34 ± 0.17	20.83 ± 0.04	1,8	45 ± 6	56 ± 5	262 ± 6	144 ± 3	30 ± 1	111 ± 5	543 ± 40	125 ± 3
208440	B1V	0.33				42 ± 7	50 ± 7	213 ± 7	92 ± 6	21 ± 1.5	100 ± 7	597 ± 65	98 ± 4
208501	B8Ib	0.75				60 ± 7	52 ± 6	255 ± 6	128 ± 6	36 ± 1	110 ± 9	666 ± 65	124 ± 4
209008	B3III	0.08				<25	<20	46 ± 6	14 ± 4	5 ± 1	15 ± 5	227 ± 40	9.5 ± 2
209975	O9Ib	0.36	21.17 ± 0.09	20.08 ± 0.09	1,6	64 ± 10	43 ± 8	258 ± 5	91 ± 5	29 ± 1.5	96 ± 8	520 ± 60	115 ± 4
210121	B3V	0.40	20.63 ± 0.15	20.75 ± 0.12	8,8	15.5 ± 3.5	<20	70 ± 7	46 ± 9	9.4 ± 0.7	27.5 ± 4	146 ± 50	25 ± 2
210839	O6If	0.57	21.15 ± 0.12	20.84 ± 0.04	1,8	52 ± 5	65 ± 5	261 ± 5	72 ± 6	31 ± 1	106 ± 5	551 ± 45	150 ± 3
212120	B6V	0.04						57 ± 7	11 ± 2.5	4.5 ± 0.8	12 ± 4	128 ± 35	9.5 ± 2
212791	B3V	0.17				23 ± 7	23 ± 6	123 ± 4	33 ± 5	12.8 ± 0.8	57 ± 5	433 ± 55	37 ± 3
214080	B1Ib	0.06	20.58 ± 0.1	18.35 ± 0.1	1,9	22 ± 7	14 ± 4	49 ± 5	23 ± 5	<4.5	29 ± 8	294 ± 60	5 ± 1.5
214680	O9V	0.11	20.69 ± 0.14	19.22 ± 0.06	1,6	<8	<27	74 ± 5	25 ± 3	5.9 ± 0.7	20 ± 5	237 ± 50	15 ± 1
214930	B2IV	0.10				<15	<12	53 ± 4	18 ± 3	7.5 ± 1.5	20 ± 5	161 ± 40	16 ± 3
215733	B1II	0.11	20.75 ± 0.09	19.45 ± 0.1	1,9	33 ± 6	24 ± 4	82 ± 5	32 ± 4	8.6 ± 1	40 ± 6	246 ± 45	21.5 ± 2
218376	B0.5IV	0.25	20.91 ± 0.09	20.15 ± 0.09	1,6	36 ± 6	45 ± 5	146 ± 8	61.7 ± 6	14.9 ± 1	55 ± 6	365 ± 45	68 ± 3
219188	B0.5II	0.13	20.75 ± 0.09	19.38 ± 0.12	1,6	16 ± 5	14 ± 4.5	70 ± 4	27 ± 4	7.2 ± 0.8	44 ± 5	370 ± 55	19 ± 3
BD+63 1964	B0II	1.00				210 ± 12	195 ± 20	729 ± 10	295 ± 9	92 ± 2	313 ± 15	1380 ± 200	330 ± 6
223385 (6 Cas)	A3Iae	0.67				85 ± 8	166 ± 15	582 ± 6	167 ± 6	35 ± 3	230 ± 8	1360 ± 70	193 ± 5
224572	B1V	0.19	20.79 ± 0.08	20.23 ± 0.09	1,6	<20	15 ± 5	78 ± 4	31 ± 4	9 ± 1	27 ± 5	276 ± 40	30 ± 3
229059	B1.5Iap	1.71				116 ± 12	96 ± 5	457 ± 7	163 ± 3	61 ± 1	212 ± 10	1090 ± 150	241 ± 5

Notes.

[a] The calculated values of E_{B-V} are based on the intrinsic colors from Johnson (1963).

[b] The references for N(H) and N(H_2), respectively. References. (1) Diplas & Savage 1994, Table 1; (2) Diplas & Savage 1994, Table 2; (3) Shull & Van Steenberg 1985, Table 1; (4) Shull & Van Steenberg 1985, Table 2; (5) Bohlin et al. 1978; (6) Savage et al. 1977; (7) Spitzer et al. 1974; (8) Rachford et al. 2002; (9) B. Rachford, unpublished; (10) Rachford et al. 2009; (11) K. Gillmon 2003, private communication; (12) Jenkins et al. 1999; (13) Jenkins et al. 2000.

with a much broader feature at λ5795. As shown in Section 3.2, we find very good correlations associated with λ6204.5 and lower ones for λ5797.1. Determining which features correlate best may prove to be a useful tool for guiding the placement of integration limits. However, it is impossible to know the correct approach in advance, so we favor systematic repeatability until the true profile can be established by species identification in the laboratory.

Also shown in Figure 1 are the DIBs identified in atlas Papers II and III (black and red tick marks), the stellar lines

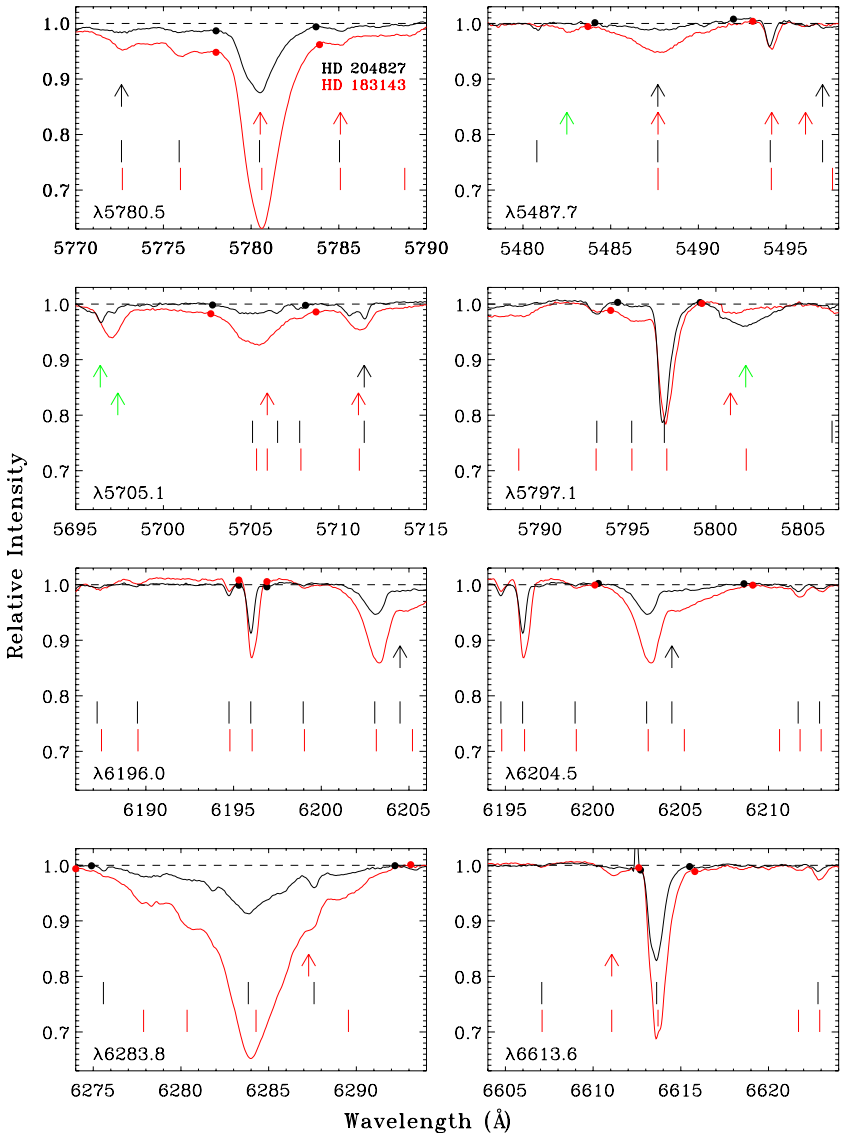

Figure 1. Continuum normalized spectral profiles of the eight DIBs toward HD 204827 (black) and HD 183143 (red). Filled circles indicate the limits of integration for calculating equivalent widths. Black arrows indicate the locations of stellar lines identified in the DIB atlas for HD 204827 (Paper II) and red arrows the stellar lines for HD 183143 (Paper III). Green arrows show additional stellar lines identified in the low-reddened comparison stars for these two stars. Note the apparent offset in LSR velocity of the DIBs in the spectra of the two stars. See the text for an explanation. The vertical scale in all panels is the same to clearly show the relative strengths of the DIBs. The spike just to the left of the λ6613.6 DIB is an artifact.

Table 2
DIB Correlation Data with log[N(H)][a,b]

DIB (FWHM[c])	Correlation Coefficient	Reduced χ^2	Number of Sight Lines	Correlation Coefficient[d]	a[e]	b[e]
5780.5 (2.11)	0.94	1.209	74	0.90	19.00 ± 0.08	0.94 ± 0.04
6283.8 (4.77)	0.89	1.250	71	0.87	17.65 ± 0.20	1.30 ± 0.07
6204.5 (4.87)	0.89	1.559	69	0.84	19.02 ± 0.11	1.12 ± 0.06
6196.0 (0.42)	0.89	2.035	68	0.79	19.90 ± 0.06	0.95 ± 0.05
6613.6 (0.93)	0.87	2.794	70	0.77	19.89 ± 0.06	0.67 ± 0.03
5705.1 (2.58)	0.83	1.278	52	0.73	19.38 ± 0.16	1.08 ± 0.09
5797.1 (0.77)	0.82	3.269	65	0.72	19.59 ± 0.09	0.85 ± 0.05
5487.7 (5.20)	0.78	1.516	55	0.60	19.28 ± 0.16	1.13 ± 0.09

Notes.
[a] All entries computed using logarithmic values of DIB equivalent widths.
[b] Data in Columns 2, 3, 4, 6, and 7 exclude ρ Oph A, θ^1 Ori C, and HD 37061.
[c] FWHM from Paper II. All wavelengths are in units of Å.
[d] Includes all sight lines.
[e] Coefficients for $\log[N(\mathrm{H})] = a + b \times \log[W_\lambda(\mathrm{DIB})]$.

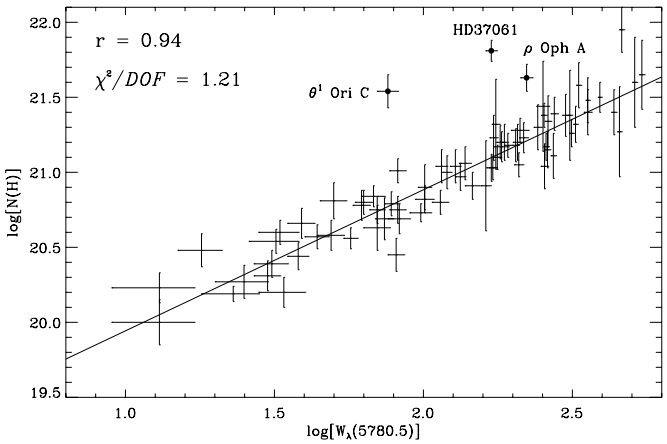

Figure 2. log[N(H)] vs. log[W_λ(5780.5)]. In this and the figures which follow, the straight line is the least-squares fit to the data excluding the outlying points, which are indicated by filled circles. The slope and intercept of the line are given in Table 2. All EWs are in units of mÅ.

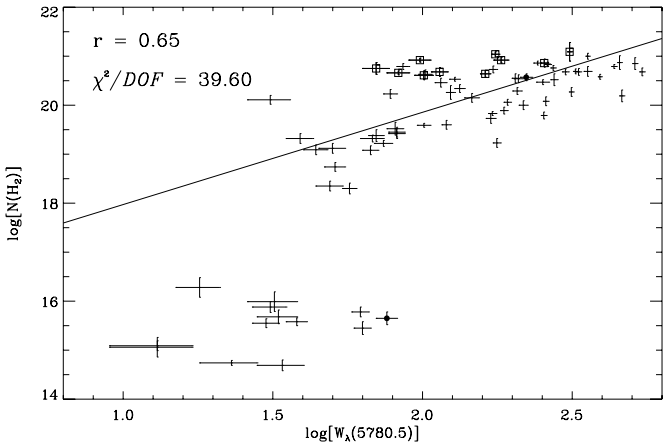

Figure 3. $N(H_2)$ vs. W_λ(5780.5). Open squares denote sight lines with molecular fraction $f(H_2) > 0.5$. The straight line is the least-squares fit to the points with $\log[N(H_2)] > 18$, and is given by $\log[N(H_2)] = (16.09 \pm 0.09) + (1.88 \pm 0.04) \times \log[W_\lambda(5780.5)]$.

(black and red arrows), and a few additional stellar lines (green arrows) observed in the spectra of the lightly reddened comparison stars. Broad DIBs, like λ6283.8, may include multiple weak DIBs identified in the atlases. The criteria for selecting the DIBs are clearly described in these papers, but no claim is made regarding whether these separate DIBs really arise from the same carrier molecule. Thus, including or excluding them is equally justified. Note that our choice to include them does not significantly affect our results. For example, the three DIBs in the wings of the HD 183143 profile have EWs of 28, 22, and 19 mÅ (Paper III) which, even in total comprise only a few percent of the 1910 mÅ EW of the main DIB. Similarly, for HD 204827 the EWs of the two flanking DIBs are 3 and 14 mÅ (Paper II), compared to 518 mÅ for the main DIB. For λ5797.1 and λ6204.5, flanking DIBs were formally identified in the atlas papers but, as noted above, we elected to include the wings in our EW measurements of the main DIBs until identifications are secure.

There are very few stellar lines blended with the DIBs considered here. Those present are generally weak. Their treatment with respect to measuring EWs is described in Papers II and III.

3.1. Correlation of λ5780.5 with N(H), N(H$_2$), and E_{B-V}

Herbig (1993) noted the strong correlation between N(H) and W_λ(5780.5). This relationship is shown in Figure 2 for our sight lines. The correlation coefficient[13] for this relationship is $r = 0.94$, when three stars are excluded from the sample: ρ Oph A, θ^1 Ori C, and HD 37061 (see Table 2). These outliers were also rejected by Herbig (1993), who noted the remarkably high radiation field of the Trapezium stars, and that both N(Na) and the DIBs λ5780.5 and λ5797.1 are low with respect to N(H). These three stars are very weak in K I (Welty & Hobbs 2001). They have very flat far-UV extinction curves and θ^1 Ori C and HD 37061, in particular, have weak 2175 Å bumps (Fitzpatrick & Massa 2007). Table 2 also includes the reduced χ^2 for a straight line fit to the plot of log(λ5780.5) versus log(N(H)), excluding these three outlying stars. The values in the fifth column of the table are the correlation coefficients when these stars are included in the sample. Table 2 also includes the correlation coefficients for the remaining DIBs with log(N(H)), as well as the coefficients of the best linear fits, excluding the same three outliers.

Figure 3 shows the relation between $N(H_2)$ and W_λ(5780.5). For the full data set it is clear that there is a very poor relationship between the two quantities, especially compared to Figure 2 for N(H) and W_λ(5780.5). It is noteworthy that stars with $N(H_2)$ ranging over a factor of more than 10^5 can have identical values of W_λ(5780.5). A special set of sight lines is denoted by open squares in Figure 3: those with fractional abundance of H_2 ($f = [2N(H_2)]/[N(H) + 2N(H_2)]$) greater than 0.5. This molecular fraction is a line-of-sight average, so the value of f for some individual clouds almost certainly must be greater than 0.5. In these clouds most hydrogen is in the form of H_2. Considering a slightly less restricted set of sight lines, those for which $\log(N(H_2)) > 18$ we find $r = 0.65$, considerably lower than the correlation coefficient of N(H) with λ5780.5. The correlation coefficients for all eight DIBs with $N(H_2)$ are given in Table 3. The reduced χ^2 values are far greater than for the DIB–log(N(H)) relations shown in Table 2.

Figure 4 shows the correlation of E_{B-V} and W_λ(5780.5). Reddening errors are difficult to quantify, but we estimate them to be approximately 0.03 mag. This plot covers a large range in E_{B-V}, from 0.01 to 3.31 mag. The three points with the highest values of E_{B-V} are Cyg OB2 12, Cyg OB2 5, and HD 229059, all of which are in the Cyg OB2 cloud.There is significant scatter in this plot, with $r = 0.82$, indicating that λ5780.5 is not directly associated with the column density of dust grains responsible for the optical differential extinction. The correlation coefficients for all eight DIBs with E_{B-V}, as well as the coefficients for the best-fit lines, are given in Table 4. Again, the reduced χ^2 values are far greater than for the DIB–log(N(H)) relations. Note that the best-fit lines have not been constrained to go through the origin in any of the plots presented in this paper.

The prominent jump in the data points in Figure 3 is at $W_\lambda(5780.5) \approx 50$ mÅ, corresponding to $E_{B-V} \approx 0.1$, according to Figure 4. This matches well the value of $E_{B-V} \approx 0.08$ that marks the beginning of a sharp transition from low to high values of $N(H_2)$ in interstellar clouds (Savage et al. 1977). This level of reddening indicates the presence of a sufficient density of dust grains to favor the formation of H_2, and a high enough

[13] All correlation coefficients in this paper refer to Pearson's correlation coefficient. The reader is cautioned that some authors (e.g., Wallerstein et al. 2007) use other statistics, such as Spearman's rank correlation coefficient.

Table 3
DIB Correlation Data with $\log[N(H_2)]$[a,b]

DIB	Correlation Coefficient	Reduced χ^2	Number of Sight Lines	Correlation Coefficient[c]
5780.5	0.65	39.60	64	0.65
6283.8	0.46	9.99	63	0.46
6204.5	0.60	24.61	63	0.60
6196.0	0.74	21.10	63	0.74
6613.6	0.80	21.82	64	0.80
5705.1	0.56	10.62	49	0.56
5797.1	0.79	14.83	63	0.79
5487.7	0.47	10.42	52	0.47

Notes.
[a] All entries computed using logarithmic values of DIB equivalent widths and only for sight lines with $\log[N(H_2)] > 18$.
[b] Data in Columns 2, 3, and 4 exclude ρ Oph A, θ^1 Ori C, and HD 37061.
[c] Includes all sight lines.

Table 4
DIB Correlation Data with E_{B-V}[a,b]

DIB	Correlation Coefficient	Reduced χ^2	Number of Sight Lines	Correlation Coefficient[c]	a[d]	b[d]
5780.5	0.82	48.44	133	0.82	$(-8.36 \pm 3.48) \times 10^{-3}$	$(1.98 \pm 0.01) \times 10^{-3}$
6283.8	0.82	16.60	127	0.82	$(-7.71 \pm 0.78) \times 10^{-2}$	$(9.57 \pm 0.17) \times 10^{-4}$
6204.5	0.83	26.71	119	0.83	$(-7.22 \pm 0.67) \times 10^{-2}$	$(5.99 \pm 0.08) \times 10^{-3}$
6196.0	0.85	25.59	117	0.85	$(-5.07 \pm 0.56) \times 10^{-2}$	$(2.11 \pm 0.02) \times 10^{-2}$
6613.6	0.84	45.27	120	0.83	$(1.96 \pm 0.37) \times 10^{-2}$	$(4.63 \pm 0.04) \times 10^{-3}$
5705.1	0.80	13.55	91	0.80	$(-1.74 \pm 0.16) \times 10^{-1}$	$(1.20 \pm 0.03) \times 10^{-2}$
5797.1	0.84	25.16	113	0.84	$(-2.86 \pm 0.57) \times 10^{-2}$	$(5.74 \pm 0.06) \times 10^{-3}$
5487.7	0.80	12.84	93	0.79	$(-6.41 \pm 1.31) \times 10^{-2}$	$(9.67 \pm 0.25) \times 10^{-3}$

Notes.
[a] All entries computed using linear values of DIB equivalent widths.
[b] Data in Columns 2, 3, 4, 6, and 7 exclude ρ Oph A, θ^1 Ori C, and HD 37061.
[c] Includes all sight lines.
[d] Coefficients for $E_{B-V} = a + b \times W_\lambda(5780.5)$.

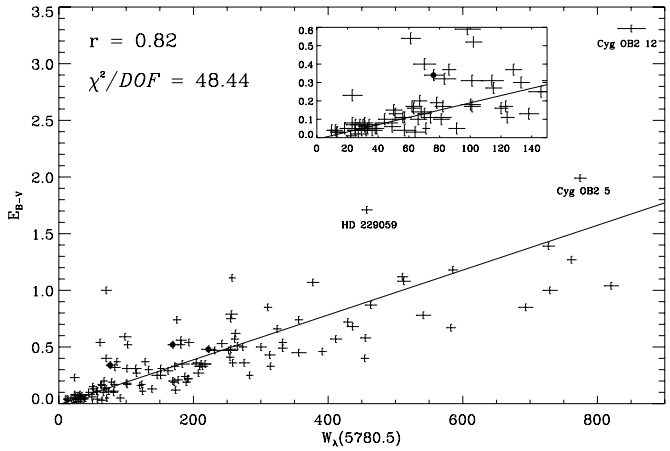

Figure 4. E_{B-V} vs. $W_\lambda(5780.5)$. The inset in this and the following correlation plots shows a close-up view of the region near the origin. The best-fit line has not been constrained to go through the origin in any of the plots in this paper.

column density of H_2 initiates self-shielding, which allows an exponential increase in $N(H_2)$.

3.2. DIB–DIB Correlations

The eight DIBs in our sample are λλ 5780.5, 6204.5, 6283.8, 6196.0, 6613.6, 5705.1, 5797.1, and 5487.7, in order of decreasing correlation coefficient with N(H). In Table 5, we give the mutual correlation coefficients between all pairs of DIBs in this study. Of the 28 pairs, 27 have correlations greater than 0.9. The exception is λλ5797.1–5487.7, with $r = 0.87$. DIBs which arise from the same carriers, or whose carriers may have been formed in the presence of a third, common carrier, would have correlation coefficients very close to unity. None of the pairs considered here have such a high correlation, with the exception of λλ6196.0–6613.6, as discussed in Paper IV.

We now consider correlations between λ5780.5 and the other seven DIBs. Correlation coefficients are given in Table 6, with the modified set, which excludes the three outlier sight lines, in Column 2, and the full set in Column 5. Note that correlations for the full and modified set are identical to within our errors. This is not true for the full and modified set for the relation between the DIBs and N(H) (Table 2). Table 6 also gives the coefficients of the best-fit lines for the DIB–$W_\lambda(5780.5)$ plots, excluding the three outliers.

Figures 5 through 11 show the relationship between λ5780.5 and the other DIBs in our sample. We note here some of the characteristics of these plots.

Figure 5 shows the λ6204.5 versus λ5780.5 relationship (correlation coefficient $r = 0.97$). The greatest outliers in terms of the number of standard deviations off the best-fit line in both the x and y directions combined, are HD 40839, HD 194839, HD 147889, AE Aur, τ CMa, and μ Sgr. However, with a correlation coefficient of 0.97, this is one of the best correlations observed, even better than λ5780.5 with N(H) ($r = 0.94$).

Figure 6 shows the correlation of the DIBs λ6196.0 and λ5780.5 ($r = 0.97$). The outliers here include 6 Cas, HD

Table 5
DIB–DIB Correlation Coefficients[a,b]

DIB	5780.5	6204.5	6196.0	6283.8	6613.6	5705.1	5797.1	5487.7
5780.5	1	0.97	0.97	0.96	0.96	0.98	0.93	0.95
6204.5	0.97	1	0.96	0.98	0.94	0.96	0.91	0.95
6196.0	0.97	0.96	1	0.93	0.99	0.93	0.96	0.94
6283.8	0.96	0.98	0.93	1	0.91	0.94	0.86	0.92
6613.6	0.96	0.94	0.99	0.91	1	0.93	0.95	0.91
5705.1	0.98	0.96	0.93	0.94	0.93	1	0.90	0.93
5797.1	0.93	0.91	0.96	0.86	0.95	0.90	1	0.87
5487.7	0.95	0.95	0.94	0.92	0.91	0.93	0.87	1

Notes.
[a] All entries computed using linear values of DIB equivalent widths.
[b] Excluding ρ Oph A, θ^1 Ori C, and HD 37061.

Table 6
Correlation Data with λ5780.5[a,b]

DIB	Correlation Coefficient	Reduced χ^2	Number of Sight Lines	Correlation Coefficient[c]	a[d]	b[d]
5705.1	0.98	2.20	91	0.98	−0.25 ± 1.07	0.228 ± 0.004
6204.5	0.97	6.92	119	0.97	−0.24 ± 0.88	0.412 ± 0.004
6196.0	0.97	11.66	116	0.97	−0.63 ± 0.17	0.111 ± 0.001
6613.6	0.96	28.05	119	0.96	−13.39 ± 0.52	0.467 ± 0.003
6283.8	0.96	3.82	125	0.96	28.24 ± 5.8	2.32 ± 0.03
5487.7	0.95	4.86	93	0.95	−2.29 ± 1.13	0.233 ± 0.005
5797.1	0.93	26.35	113	0.93	−1.65 ± 0.72	0.384 ± 0.003

Notes.
[a] All values computed using linear values of DIB equivalent widths.
[b] Data in Columns 2, 3, 4, 6, and 7 exclude ρ Oph A, θ^1 Ori C, and HD 37061.
[c] Includes all sight lines.
[d] Coefficients for $W(\mathrm{DIB}) = a + b \times W_\lambda(5780.5)$.

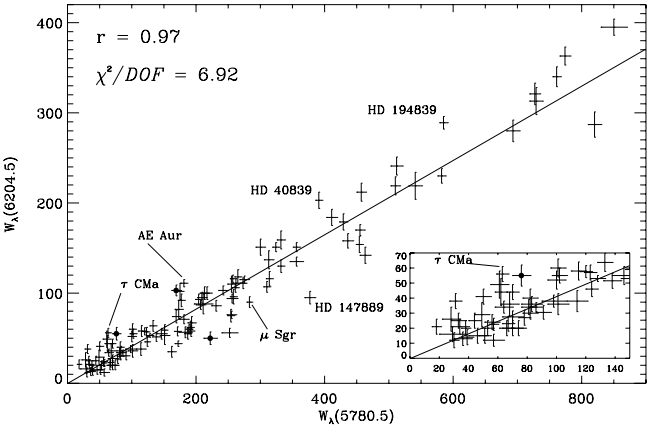

Figure 5. $W_\lambda(6204.5)$ vs. $W_\lambda(5780.5)$.

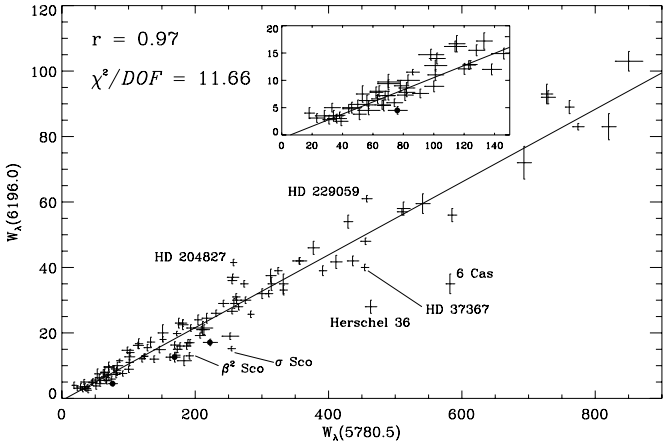

Figure 6. $W_\lambda(6196.0)$ vs. $W_\lambda(5780.5)$.

204827, σ Sco, Herschel 36, HD 37367, HD 229059, and β^2 Sco. The reduced χ^2 is almost 12 (Table 6), indicating a rather large scatter of data points, even though they are highly correlated.

The λ6283.8 versus λ5780.5 correlation ($r = 0.96$) in Figure 7 has only two points that are more than 5σ off the best-fit line in both the x and y directions, ϵ Cas and HD 147889. Other outliers include HD 157857, HD 169454, HD 194839, and HD 219188. λ6283.8 is by far the strongest of the eight DIBs but there is no evidence of saturation in Figure 7.

Figure 8 plots λ6613.6 versus λ5780.5 ($r = 0.96$). This relation has a reduced χ^2 of more than 28, the highest of all DIB–$W_\lambda(5780.5)$ pairs (Table 6). Among the points which deviate the most are HD 204827, HD 194839, ϵ Cas, HD 37367, 6 Cas, and HD 166734.

Figure 9 plots λ5705.1 versus λ5780.5 ($r = 0.98$). This relation has the highest correlation coefficient and the lowest scatter ($\chi^2 = 2.2$) of any of our DIB pairs. No point deviates from the best-fit line in the $W_\lambda(5705.5)$ direction by more than 4σ. The largest outliers are 6 Cas, HD 30614, HD 206773, HD 157857, X Per, and HD 194839. The correlation coefficient is comparable to that of the λλ6196.0 − 6613.6 pair discussed in Paper IV, and will be subject to additional, detailed study by our group.

The λ5797.1 versus λ5780.5 plot ($r = 0.92$), Figure 10, also exhibits high scatter, with reduced χ^2 exceeding 26. We notice a group of points falling below the line near $W_\lambda(5780.5) =$ 175 mÅ. This includes HD 53975 at $(x, y) = (177,26)$, HD

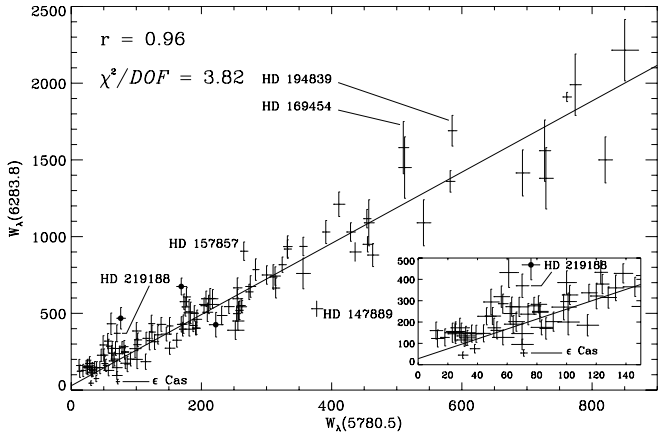

Figure 7. $W_\lambda(6283.8)$ vs. $W_\lambda(5780.5)$.

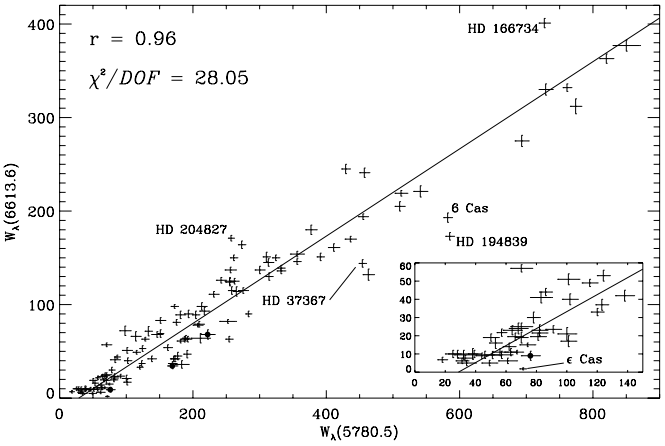

Figure 8. $W_\lambda(6613.6)$ vs. $W_\lambda(5780.5)$. This shows most clearly the threshold effect—some minimum amount of λ5780.5 must be present before λ6613.8 begins to appear.

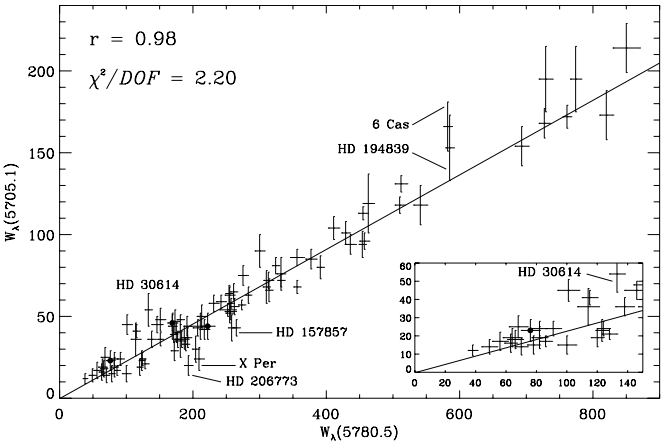

Figure 9. $W_\lambda(5705.1)$ vs. $W_\lambda(5780.5)$. This has the smallest reduced χ^2 and the highest correlation coefficient of the DIBs with respect to λ5780.5.

37903 at (183,33), β^2 Sco at (191,36), ω^1 Sco at (192,40), ν Sco AB at (187,49), and β^1 Sco AB at (171,34). Other outliers include HD 204827, HD 172028, Herschel 36, and 6 Cas.

The λ5487.7 versus λ5780.5 plot ($r = 0.95$), shown in Figure 11, exhibits a group of points sitting above the line at both the lowest and the highest column densities. The first group includes HD 201345 at (100,46), HD 186994 at (101,40), ζ Per at (98,22), o Per at (101,31), 40 Per at (115,33), ϕ^1 Ori at (68,29),

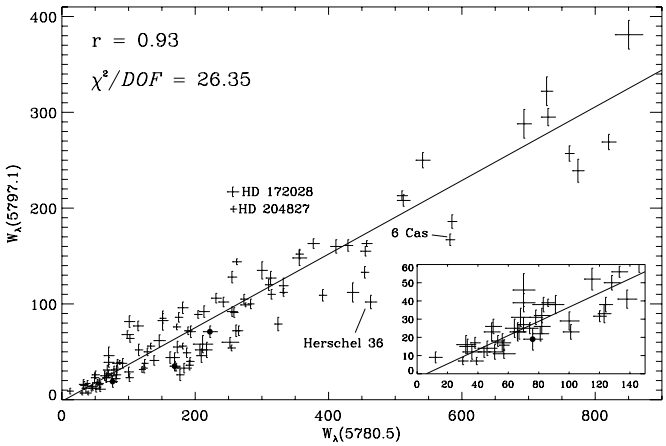

Figure 10. $W_\lambda(5797.1)$ vs. $W_\lambda(5780.5)$.

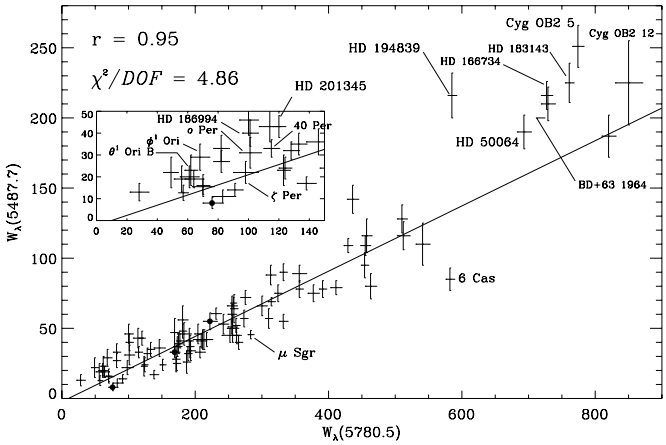

Figure 11. $W_\lambda(5487.7)$ vs. $W_\lambda(5780.5)$.

and θ^1 Ori B at (61,20). The second group includes HD 194839, HD 166734, HD 183143, Cyg OB2 5, Cyg OB2 12, BD+63 1964, and HD 50064. The two largest outliers below the line are 6 Cas and μ Sgr. This is the only DIB–DIB plot for which there is a possible systematic deviation from a linear relationship at high column densities. In this case, λ5780.5 may be saturating at $W_\lambda \gtrsim 600$ mÅ. However, no saturation is indicated at similar line strengths in the correlations with other DIBs, so it is unlikely that this is the cause of this distribution of points. If this is correct, it implies that λ5487.7 is getting stronger per H atom for high levels of λ5780.5.

4. DISCUSSION

Most interstellar quantities will show a positive correlation with each other simply due to the increase of interstellar material with distance. This is most clearly reflected in the correlation of DIBs with extinction. For the eight DIBs considered here the correlation coefficients with E_{B-V} range from 0.80 to 0.85 (Table 4), with an average of 0.82. Thus, we may regard $r \sim 0.86$–0.88 as the minimum required to indicate that two quantities are physically correlated at a significant level.

By this measure λ5780.5 is the only DIB in our study that is unambiguously well-correlated with N(H), and even in this case the outlier points (Figure 2) are prominent exceptions. These three stars have in common the presence of strong local radiation fields. Noticing that the outliers have particularly low abundances of λ5780.5 relative to their H column densities

compared to the general correlation, a possible explanation is that the radiation fields in these regions are hard enough to destroy the carrier of λ5780.5, and that local radiation generally regulates DIB abundances, which are likely characterized by distinct critical wavelengths of ionizing radiation. Because all of the DIBs are well correlated with λ5780.5, with correlation coefficients 0.92–0.97 (Table 5), but only λ5780.5 is very well correlated with N(H) (Table 2), we infer that the critical energy for regulating λ5780.5 is similar to the energy that regulates the H abundance, and greater than that of the other DIBs. We note that the destruction mechanism may be simple ionization, but it could also be dissociation. However, the apparent destruction effect in the presence of significant photon fluxes indicates that the λ5780.5 carrier might be an ion.

These conclusions are supported by Sonnentrucker at al. (1997), who examined the ionization properties of the DIBs λλ5780.5, 5797.1, 6379.3, and 6613.6. They conclude that the carriers of these DIBs are separate gas-phase molecules. By comparing W_λ/E_{B-V} as a function of E_{B-V} for each DIB, they find that λ5780.5 reaches its maximum at the lowest value of E_{B-V}, indicating that the carrier of this DIB is the most resistant of the four DIB carriers to strong UV fields.

While the main interstellar clouds in the three outlier sight lines are subject to higher than average radiation fields, they are not the only stars in our sample with this property. The Na I and K I lines in the two Trapezium sight lines, θ^1 Ori C and HD 37061, are exceptionally weak, relative to N(H). ρ Oph A, however, is a bit puzzling. Various Sco-Oph sight lines (and some others in other regions) exhibit relatively weak Na I and K I (Welty & Hobbs 2001). For these targets only ρ Oph A is among the most discrepant in λ5780.5 versus N(H), but most other Sco-Oph sight lines tend to be deficient in λ5780.5, as well. Unfortunately, we do not have a good quantitative measure of radiation field strength in many cases. One can use the higher H_2 rotational level populations ($J = 4, 5$) to estimate this, but the column densities of those levels are often very hard to determine accurately because the lines are generally on the flat part of curve of growth for most sight lines of interest here. We have no measure of H_2 toward HD 37061 and the higher J lines have not been reported toward ρ Oph A. The error on $N(H_2)$ toward θ^1 Ori C is among the largest in our sample. Obtaining more extensive data on the strength of the radiation fields along a large number of sight lines would be a very interesting study.

If two DIBs are formed from transitions between a single ground state and two different vibronic levels, their measured strengths should be perfectly correlated, with a correlation coefficient of unity. This is not quite true even for the best observed DIB–DIB correlation, λ6196.0 versus λ6613.6. McCall et al. (Paper IV) explore this particular pair and discuss the possibility that the true errors are underestimated. The most likely causes of such a situation are: (1) there are errors in continuum placement, (2) there are blends of DIBs that are not physically related, and (3) there is uncorrected contamination from telluric water vapor lines. The first of these could be especially true for λ5780.5, which is superimposed on a much wider feature centered at 5778 Å (Herbig 1975; see also the combined spectral plots shown in Figure 11 of Papers II and III). Without knowing the origin of the features that make up this blend (Krelowski et al. 1997), it is hard to evaluate this effect. For the much narrower λ5797.1 DIB the second effect may be operative. The feature is multiple and the line shapes differ from star to star in our data (see Figure 1). We suspect the short wavelength contribution to this DIB is a C_2 DIB (Paper I), while the long wavelength component is more closely related to λ5780.5. This explanation is consistent with the well-known $\sigma - \zeta$ effect of 5780.5 and 5797.1: in the prototype "σ" sight line, σ Sco, λ5780.5 is much deeper than λ5797.1, while in the prototype "ζ" sight line, ζ Oph, the depths of the two lines are comparable (Krelowski & Sneden 1995). The stars with high $N(H_2)$ and low W_λ(5780) are all ζ-type stars, including strong C_2 DIBs, and produce a deep blueward component of the proposed C_2 DIB at 5797.1 Å.

The $\sigma - \zeta$ effect might be more of a geometrical effect than an ionization effect. It is well-known that λ5780.5 is poorly correlated with trace neutral species, such as K I and Na I (Welty et al. 2006). This is also true of other σ-type DIBs that are best correlated with N(H), such as λλ6283.8, 6204.5. On the other hand, the ζ-type DIB λ5797.1 is better correlated with the trace neutrals (Galazutdinov et al. 2004). These neutrals predominantly exist in the cores of clouds, which provide adequate shielding of the UV field, and where high molecular fractions of H_2 exist due to self-shielding. These results are consistent with the σ-type DIBs existing in the outer regions of clouds and the ζ-type DIBs existing deep in the interior of the clouds. The variable strength ratio of λλ5780.5, 5797.1 has been discussed by several authors, such as Krelowski et al. (1997). λ5797.1 has the lowest correlation coefficient ($r = 0.93$) with λ5780.5 of any of the DIBs in our study (Table 6), even though it still exceeds the value expected from the general growth of interstellar material, as noted above.

Most of our sight lines penetrate multiple clouds and therefore average out these effects. Cami et al. (1997) studied 13 stars with only single clouds along the lines of sight. They confirm the classification of DIBs into four different families, including σ and ζ. However, the most convincing evidence of this hypothesis will come from mapping several clouds spatially by observing multiple stars at various locations behind the clouds. Correlations among DIBs and with neutral atoms and with molecules, such as H_2, C_2, CN, and CH will indicate whether the geometrical interpretation is correct. This is the subject of a future study by our group.

Examination of DIBs that fall in the clean parts of the spectra of a number of stars indicate the presence of a number of interstellar absorption components. Galazutdinov et al. (2002a, 2005) argue that most strong DIBs have structure. While these authors conclude the structures are evidence of the R, P, Q rotational structure of molecules of modest size, our study suggests that blends of unrelated DIBs may be the origin of structure in some cases.

The question of what features in the neighborhood of the main DIB to include in the measurements of EW is difficult. We do not have the fine spectral resolution of Galazutdinov et al. (2002a) and cannot separate the blended features in two of our DIBs, λ5797.1 and λ6204.5, but we have a larger data set at very high S/N. It is difficult even at high resolution to conclude whether lines have structure due to multiple components along a line of sight, blends of unrelated species, or structure from energy levels in a common carrier. Even if we know in advance that DIBs from two different carriers are involved, we still do not know what profiles to use in the deconvolution fitting process. We therefore measure the full EW of the blends. Figure 1 shows that the two features in the profile of λ6204.5 approximately scale with each other, and this DIB has among the highest correlation coefficients with the other DIBs (Table 5) and with N(H) (Table 2), and the correlation with λ5780.5 has low χ^2 (Table 6). In contrast, the features of λ5797.1 do not scale with each other, this DIB has low correlation coefficients with the

other DIBs and N(H), and the correlation with λ5780.5 has very high χ^2. It would appear that the two features blended in the λ6204.5 feature we measure as one feature are either from the same carrier or from two separate carriers that are almost perfectly correlated. As previously noted, such considerations may help guide the correct placement of limits in future studies.

Examination of Table 6 shows that the intercepts of the best-fit lines pass through the origin for the correlation of λ5780.5 with DIBs λλ5705.1, 6204.5, 5487.7, and possibly λλ5797.1 and 6196.0. However, our data show that this is not true for λ6283.8, and especially λ6613.6. This may be evidence of a threshold effect, such that a substantial amount of 5780.5 must be produced before 6613.6 can begin to form. Since N(H) is very well correlated with λ5780.5, this implies that some minimum column density of H is required before the appearance of some DIBs becomes evident.

Figure 7 shows a possible threshold in the opposite sense. This is the only case in which the linear fit has a statistically significant positive intercept, indicating that 6283.8 appears before 5780.5. In addition, below $W_\lambda(5780.5) \approx 150$ mÅ there are significantly more points above the best-fit line than below. Below $W_\lambda(5780.5) \approx 50$ mÅ the distribution flattens, with $W_\lambda(6283.8)$ remaining approximately constant as $W_\lambda(5780.5)$ decreases. This may be caused by two effects. (1) 6283.8 is among the broadest DIBs in this study (FWHM = 4.77 Å, Table 2), making continuum fitting somewhat less reliable than for narrower DIBs. (2) There is considerable telluric contamination in such a wide DIB and our nightly blanket correction for telluric lines (Section 2) may introduce unrecognized errors. Indeed, we estimate our minimum detectable DIB EW to be approximately 150 mÅ, about the same as the plateau in Figure 7. This line is asymmetric and far from Gaussian in shape, so it would not be evident from an inspection of the line profile if one or more interfering lines are present.

One of the most useful results of this work is the ability to estimate the total column density of atomic hydrogen along a Galactic sight line based on a measurement of the EW of a single DIB. The tight correlation between N(H) and $W_\lambda(5780.5)$ shown in Figure 2 demonstrates that this technique can be used in most cases, and in fact this has a higher correlation coefficient and lower χ^2 than E_{B-V} versus N(H). However, the relationship fails to hold for the outlier stars, so care must be taken if the sight line passes through a region of high UV-radiation, assuming this influences the abundance of the DIB carriers, as discuss above. A second empirical application is to compare the correlations presented here with correlations among the same features in other galaxies, in hopes that differences can be related to different physical properties of the galaxies and lead to an explantion of the DIBs. For example, note that since N(CH) and $N(H_2)$ are moderately well correlated (Welty et al. 2006), the total H (atomic plus molecular) column density can be estimated for stars too faint to have measured far UV extinction curves.

Welty et al. (2006) examined the strengths of the λλ5780.5, 5797.1, and 6283.8 DIBs toward a relatively small number of stars in the Magellanic Clouds. They found that the correlations of these with N(H) were lower than with E_{B-V}, which is not true for most of the DIBs in the current study. They also found that these DIBs are systematically weaker relative to N(H) than they are in the Milky Way by factors of 7–9 (in the LMC) and ∼20 (in the SMC), and weaker by about a factor of 2 relative to E_{B-V}. In a slightly larger sample of stars with improved N(H) for some sight lines, D. E. Welty et al. (2011, in preparation) find that the correlations are slightly better than those reported in the earlier study but still not as good as ours for Galactic sight lines. These differences may be due to lower metallicities or stronger radiation fields found in the clouds; see Welty et al. (2006) for additional discussion of these points.

5. SUMMARY

We have used a large database of high signal to noise ratio spectra of 133 stars to perform one of the most extensive comparisons to date between strengths of DIB pairs and between DIBs and N(H), $N(H_2)$, and E_{B-V}. We have presented linear fit parameters and correlation coefficients for these relationships. We reach the following conclusions.

1. Only one DIB in our study, λ5780.5, is unambiguously well-correlated with N(H), in the sense that the correlation coefficient exceeds what one would expect from the growth of interstellar material with distance.
2. None of the DIB–DIB correlation coefficients considered here are high enough to conclude that any pair arises from the same carrier. However, as described in Paper IV, the λλ6196.0–6613.6 pair may be perfectly correlated if the errors were underestimated by a small amount. The correlation of the λλ5780.5–5705.1 DIBs is also very high and further study is warranted.
3. Seven of the eight DIBs, excepting λ5487.7, are better correlated with N(H) than with E_{B-V}.
4. All eight DIBs are very poorly correlated with $N(H_2)$. Even when we restrict the sight lines to those with $\log[N(H_2)] > 18$, the correlations are poor. At a single value of $W_\lambda(5780.5)$ the column density of H_2 can vary by a factor of 10^5. This occurs just at the level of reddening corresponding to the formation of enough H_2 to permit self-shielding.
5. The excellent correlation of λ5780.5 versus N(H) may be understood if the critical energy of radiation needed to ionize the two species is similar. The greater the flux of H ionizing radiation, the higher the degree of ionization of the λ5780.5 DIB carrier.
6. Most of the linear fits to the DIB–DIB correlations pass through the origin. This is not true for λλ6283.8 and 6613.6. This may be due to continuum placement errors, the presence of interfering DIBs, improperly corrected telluric contamination, or a threshold effect, in which one DIB cannot form until a significant amount of another DIB is present.
7. One of the most practical uses of the results presented here is the ability to estimate N(H) in Galactic sight lines based on a measurement of the EW of λ(5780.5). One must be careful to exclude sight lines in high radiation environments since these maybe responsible for the outliers in this otherwise tight relationship. In addition, the correlations presented here may be compared to correlations found in other galaxies, and this may help identify the carriers of DIBs.

This work is based on observations obtained with the Apache Point 3.5 m telescope, which is owned and operated by the Astrophysical Research Consortium. We thank Tom Fishman for help with an early version of this paper and T. Oka for many useful conversations and insights into the nature of DIBs. T.P.S. was supported by NASA grant NNX08AC14G. B.J.M. gratefully acknowledges support from the David and Lucile Packard Foundation and the University of Illinois. Partial support provided by NASA contract NAS 5-26555.

REFERENCES

Allain, T., Leach, S., & Sedlmayr, E. 1996, A&A, 305, 616
Bohlin, R. C., Savage, B. D., & Drake, J. F. 1978, ApJ, 224, 132
Cami, J., Sonnentrucker, P., Ehrenfreund, P., & Foing, B. H. 1997, A&A, 326, 822
Cossart-Magos, C., & Leach, S. 1990, A&A, 233, 559
Danks, A. C., & Lambert, D. L. 1976, MNRAS, 174, 571
Diplas, A., & Savage, B. D. 1994, ApJS, 93, 211
Douglas, A. E. 1977, Nature, 269, 130
Fitzpatrick, E. L., & Massa, D. 2007, ApJ, 663, 320
Galazutdinov, G., Han, I., & Krelowski, J. 2005, ApJ, 629, 299
Galazutdinov, G., LoCurto, G., & Krelowski, J. 2008, ApJ, 682, 1076
Galazutdinov, G., Manicò, G., Pirronello, V., & Krelowski, J. 2004, MNRAS, 355, 169
Galazutdinov, G., Moutou, C., Musaev, F., & Krelowski, J. 2002a, A&A, 384, 215
Galazutdinov, G., Stachowska, W., Musaev, F., Moutou, C., Lo Curto, G., & Krelowski, J. 2002b, A&A, 396, 987
Heger, M. L. 1922, Lick Obs. Bull., 337, 141
Herbig, G. H. 1975, ApJ, 196, 129
Herbig, G. H. 1993, ApJ, 407, 412
Herbig, G. H. 1995, ARA&A, 33, 19
Herbig, G. H., & Soderblom, D. R. 1982, ApJ, 252, 610
Hobbs, L. M., et al. 2008, ApJ, 680, 1256 (Paper II)
Hobbs, L. M., et al. 2009, ApJ, 705, 32 (Paper III)
Jenkins, E. B., Tripp, T. M., Woźniak, P. R., Sofia, U. J., & Sonneborn, G. 1999, ApJ, 520, 182
Jenkins, E. B., Woźniak, P. R., Sofia, U. J., Sonneborn, G., & Tripp, T. M. 2000, ApJ, 538, 275
Jenniskens, P., & Désert, F.-X. 1994, A&AS, 106, 39
Johnson, H. L. 1963, in Basic Astronomical Data, ed. K. A. Strand (Chicago, IL: Univ. Chicago Press), 214
Josafatsson, K., & Snow, T. P. 1987, ApJ, 319, 436
Krelowski, J., Beletsky, Y., Galazutdinov, G. A., Kolos, R., Gronowski, M., & LoCutro, G. 2010, ApJ, 714, L64
Krelowski, J., Schmidt, M., & Snow, T. P. 1997, PASP, 109, 1135
Krelowski, J., & Sneden, C. 1993, PASP, 105, 1141
Krelowski, J., & Sneden, C. 1995, in The Diffuse Interstellar Bands, ed. A. G. G. M. Tielens & T. P. Snow (Astrophys. Space Science Library Vol. 202; Dordrecht: Kluwer), 13
Krelowski, J., & Walker, G. A. H. 1987, ApJ, 312, 860
Leach, S. 1995, in The Diffuse Interstellar Bands, ed. A. G. G. M. Tielens & T. P. Snow (Astrophys. Space Science Library, Vol. 202; Dordrecht: Kluwer), 281
McCall, B. J., Thorburn, J., Hobbs, L. M., Oka, T., & York, D. G. 2001, ApJ, 559, L49
McCall, B. J., York, D. G., & Oka, T. 2000, ApJ, 531, 329
McCall, B. J., et al. 2010, ApJ, 708, 1628 (Paper IV)
Merrill, P. W. 1936, ApJ, 83, 126
Motylewski, T., et al. 2000, ApJ, 531, 312
Moutou, C., Krelowski, J., d'Hendecourt, L., & Jamroszczak, J. 1999, A&A, 351, 680
Oka, T., Thorburn, J., McCall, B. J., Friedman, S. D., Hobbs, L. M., Sonnentrucker, P., Welty, D. E., & York, D. G. 2003, ApJ, 582, 823
Porceddu, I., Benvenuti, P., & Krelowski, J. 1991, A&A, 248, 188
Rachford, B. L., et al. 2002, ApJ, 577, 221
Rachford, B. L., et al. 2009, ApJS, 180, 125
Salama, F., Bakes, E. L.O, Allamandola, L. J., & Tielens, A. G. G. M. 1996, ApJ, 458, 621
Salama, F., Galazutdinov, G. A., Krelowsi, J., Allamandola, L. J., & Musaev, F. A. 1999, ApJ, 526, 265
Sarre, P. J., Miles, J. R., Kerr, T. H., Hibbins, R. E., Fossey, S. J., & Somerville, W. B. 1995, MNRAS, 277, L41
Savage, B. D., Bohlin, R. C., Drake, J. F., & Budich, W. 1977, ApJ, 216, 291
Shull, J. M., & Van Steenberg, M. E. 1985, ApJ, 294, 599
Smith, W. H., Snow, T. P., & York, D. G. 1977, ApJ, 218, 124
Sneden, C., Gehrz, R. D., Hackwell, J. A., York, D. G., & Snow, T. P. 1978, ApJ, 223, 168
Snow, T. P. 1995, in The Diffuse Interstellar Bands, ed. A. G. G. M. Tielens & T. P. Snow (Astrophys. Space Science Library Vol. 202; Dordrecht: Kluwer), 325
Snow, T. P. 2001, Spectrochim. Acta, 57, 615
Snow, T. P., York, D. G., & Welty, D. E. 1977, AJ, 82, 113
Sonnentrucker, P., Cami, J., Ehrenfreund, P., & Foing, B. H. 1997, A&A, 327, 1215
Sonnentrucker, P., Foing, B. H., Breitfellner, M., & Ehrenfreund, P. 1999, A&A, 346, 936
Spitzer, L., Cochran, W. D., & Hirshfeld, A. 1974, ApJS, 28, 373
Thorburn, J. A., et al. 2003, ApJ, 584, 339 (Paper I)
Tuairisg, S. O., Cami, J., Foing, B. H., Sonnentrucker, P., & Ehrenfreund, P. 2000, A&AS, 142, 225 (Paper I)
Tulej, M., Kirkwood, D. A., Pachkov, M., & Maier, J. P. 1998, ApJ, 506, L69
Wallerstein, G., Sandstrom, K., & Gredel, R. 2007, PASP, 119, 1268
Wampler, E. J. 1963, ApJ, 137, 1071
Wampler, E. J. 1966, ApJ, 144, 921
Wang, S., et al. 2003, Proc. SPIE, 4841, 1145
Welty, D. E., Federman, S. R., Gredel, R., Thorburn, J. A., & Lambert, D. L. 2006, ApJS, 165, 138
Welty, D. E., & Hobbs, L. M. 2001, ApJS, 133, 345
Weselak, T., Fulara, J., Schmidt, M. R., & Krelowski, J. 2001, A&A, 377, 677
Weselak, T., Galazutdinov, G. A., Musaev, F. A., & Krelowski, J. 2004, A&A, 414, 949
Weselak, T., Galazutdinov, G. A., Musaev, F. A., & Krelowski, J. 2008, A&A, 484, 381
Westerlund, B. E., & Krelowski, J. 1989, A&A, 218, 216
Wu, C-C, York, D. G., & Snow, T. P. 1981, AJ, 86, 755